



A STUDY ON THE ENERGY APPROACH DESIGN OF BASE-ISOLATED STRUCTURES

MINEO TAKAYAMA and KEIKO MORITA

Department of Architecture, Faculty of Engineering
Fukuoka University
8-19-1 Nanakuma, Jonan-ku, Fukuoka-shi 814-80 JAPAN

ABSTRACT

This paper presents the characteristics of the dynamic response of base-isolated structures by response analysis, and the validity of the prediction method based on the energy balance is discussed in comparison with the analyzed response values. The acceleration response of base isolated structures does not amplify and is below half in the fixed base structures. The energy based prediction method is very useful and valid especially for the stiffer superstructure in comparison to the stiffness of isolating story.

KEY WORDS

Seismic Isolation, Energy Based Design, Dynamic Response Analysis, Rubber Bearing, Energy Spectrum

INTRODUCTION

In base-isolated structures, the majority of energy input from an earthquake is absorbed by isolators (rubber bearings) and dampers (energy absorption mechanism) installed in a particular story (called an isolating story). Therefore, the superstructure is not required to absorb the energy, which is one of its function in conventional structural design. Moreover, the performance of isolators and dampers can be precisely measured by tests using actual size specimens. Base-isolated structures, then, represent a very simple structural system. Based on the balance between energy input from earthquakes and energy absorption by isolators and dampers, response prediction methods and safety verification methods have been established for base-isolated structures (Akiyama, 1985, 1989, Kitamura *et al.* 1992a). The total energy input, E , due to an earthquake is presented by the energy spectrum. The energy spectrum shows the relationship between the equivalent velocity V_E and the period T . The equivalent velocity V_E is defined as follows:

$$V_E = \sqrt{2E/M} \quad \text{where, } M : \text{Total mass of superstructure} \quad (1)$$

The $V_E - T$ relation can be depicted by the bi-linear type which is the envelope passing through the $V_E - T$ relation of the linear damped system with $h = 0.1$ (Akiyama, 1985). In this paper, the applicability of the energy-balancing response prediction methods is investigated by the use of the dynamic response analysis. Furthermore, the safety margin of base-isolated structures is verified by the dynamic analysis using the unexpected input ground motions. The analytical model is from 5 to 25 stories model in order to examine the effect of the height of the building on the isolation performance. The input waves used in the analysis are the artificial waves.

ENERGY BASED DESIGN

The base-isolated buildings have isolators and dampers installed in the first story. The isolators and dampers alone absorbed the earthquake energy; the superstructure does not play a part in energy dissipation. The following equation

shows the energy balance where time is t .

$$W_e(t) + W_p(t) = E(t) \quad (2)$$

where, $W_e(t)$: Strain energy of isolators, $W_p(t)$: Absorbed energy of dampers, $E(t)$: Energy input due to earthquake. Eq.(2) must also be valid when the isolating story experiences maximum deformation. If the time, when the maximum deformation occurs, is $t = t_m$, then:

$$W_e(t_m) + W_p(t_m) = E(t_m) \quad (3)$$

Generally, in structural systems with sufficiently advanced plasticity, $E(t_m) \leq E(t_0)$; t_0 is the duration of the earthquake motion. Therefore, $E(t_m)$ of Eq.(3) can be replaced by the total energy input $E(t_0)$ in the earthquake resistance evaluation of structures. If the isolators have the non-linear restoring force characteristics with no hysteresis loop and the dampers have the perfect elasto-plastic characteristics (Fig.1), their absorbed energy at $t = t_m$ can be expressed by the following equations:

$$W_e(t_m) = \frac{1}{2} K_1 \delta_{\max}^2 + \frac{1}{2} \sum_{i=2} (K_i - K_{i-1}) (\delta_{\max} - \delta_{i-1})^2, \quad W_p(t_m) = {}_s Q_y \cdot {}_s \delta_p \quad (4)$$

where, K_i : Sum of isolator's horizontal stiffness, δ_i : Changing deformation of K_i , δ_{\max} : Maximum deformation of the isolating story, ${}_s Q_y$: Sum of damper's yield shear force, ${}_s \delta_p$: Cumulative plastic deformation

The relationship of the cumulative plastic deformation ${}_s \delta_p$ to the maximum deformation δ_{\max} at $t = t_m$ is expressed as follows:

$${}_s \delta_p = \kappa \delta_{\max} \quad (5)$$

The constant value κ varied depending on the characteristics of the isolating story and input seismic wave etc. Akiyama (1989,1992a) proposed $\kappa = 8$ based on the results of the parametric dynamic analysis. The total energy input, $E(t_0)$, due to an earthquake is expressed by $E(t_0) = MV_{ET}^2 / 2$ using the equivalent velocity value $V_{ET} = V_E(t_0)$. Akiyama *et al.* (1992b) shows the design energy spectrum. This spectrum indicates the relationship between the equivalent velocity and the first period of a system for each soil type. In almost all cases, the first period for base-isolated structures is 2 seconds or more; in this range the spectrum shows the constant values. The energy input amounts V_{ET} that should be considered for this period range are varied with the soil type from 120cm/s to 300cm/s. By substituting Eqs.(4)(5) into Eq.(3), the energy balance of isolating story is expressed as follows:

$$K_1 \cdot \delta_{\max}^2 + \sum_{i=2} (K_i - K_{i-1}) (\delta_{\max} - \delta_{i-1})^2 + 2\kappa \cdot {}_s Q_y \cdot \delta_{\max} - MV_{ET}^2 = 0 \quad (6)$$

Eq.(6) is a quadratic equation of δ_{\max} , and δ_{\max} is determined by solving Eq.(6). The shear force coefficient α_s and α_f of the damper and isolator, respectively, are defined by the following equations:

$$\alpha_s = {}_s Q_y / Mg, \quad \alpha_f = {}_f Q_{\max} / Mg \quad (7)$$

where, g : Acceleration of gravity, ${}_f Q_{\max}$: Maximum shear force of isolator

The base shear force coefficient α_1 , with isolator's and damper's shear force coefficient added:

$$\alpha_1 = \alpha_f + \alpha_s \quad (8)$$

If the dampers are absent and the superstructure is rigid, the isolated period T_f is as follows:

$$T_f = 2\pi \sqrt{M/K_1} \quad (9)$$

If the maximum deformation falls in the linear range of isolator ($\delta_{\max} \leq \delta_1$), the relationship between the shear force

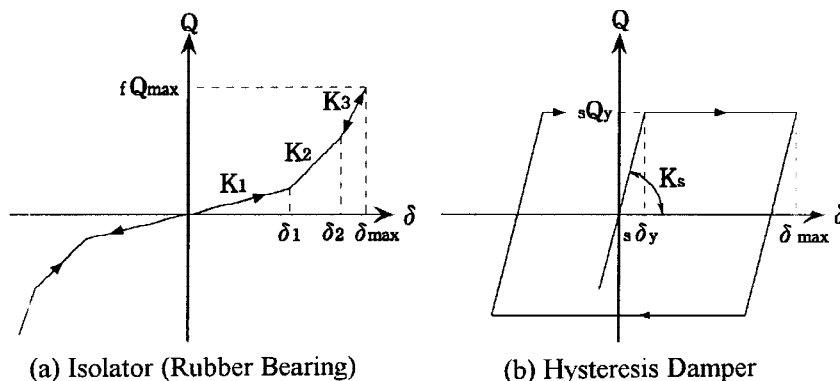


Fig.1 Restoring Force Characteristics of Isolating Story

coefficient α_s , α_1 and the maximum deformation δ_{max} can be expressed considering $\kappa = 8$ as follows:

$$\alpha_s = \frac{V_{ET}^2}{16g\delta_{max}} - \frac{\pi^2\delta_{max}}{4gT_f^2}, \quad \alpha_1 = \frac{4\pi^2\delta_{max}}{gT_f^2} + \alpha_s = \frac{V_{ET}^2}{16g\delta_{max}} + \frac{15\pi^2\delta_{max}}{4gT_f^2} \quad (10)$$

From the Eq.(10), the main parameters governing the response of base-isolated structures are the isolated period T_f , the damper's yield shear force coefficient α_s and the maximum allowable deformation δ_{max} . Fig. 2 and Fig. 3 show the relationship of $\alpha_1 - \delta_{max}$ and the relationship of $\alpha_1 - \alpha_s$ obtained from Eq.(10) at $V_{ET} = 150cm/s$. The base shear force coefficient α_1 decreases as the period T_f lengthens. The deformation δ_{max}^{opt} that minimizes the base shear force coefficient α_1 , increases along with the period T_f . However, the maximum deformation would be no more than around 40-50cm even with $V_{ET} = 300cm/s$. From these figures, the combination of the parameters governing the response can be easily grasped. The deformation δ_{max}^{opt} is derived by differentiating Eq.(10):

$$\delta_{max}^{opt} = \frac{T_f \cdot V_{ET}}{2\sqrt{15}\pi} \quad (11)$$

Substituting Eq.(11) into Eq.(10), the optimum value of α_s , α_f and α_1 are expressed as follows:

$$\alpha_s^{opt} = \frac{7\pi}{4\sqrt{15}g} \cdot \frac{V_{ET}}{T_f}, \quad \alpha_f^{opt} = \frac{8\pi}{4\sqrt{15}g} \cdot \frac{V_{ET}}{T_f}, \quad \alpha_1^{opt} = \frac{15\pi}{4\sqrt{15}g} \cdot \frac{V_{ET}}{T_f} \quad (12)$$

These equations indicate that the minimum value of the shear force coefficient of the isolating story is determined by the isolated period T_f only.

ANALYTICAL MODEL

Superstructure

The targets are uniform buildings with a longitudinal direction of two spans and a transverse direction of five spans, as shown in Fig.4. The floor area of each story is $700m^2$ ($35m \times 20m$), weight per unit of floor area is $1.4t/cm^2$. Each

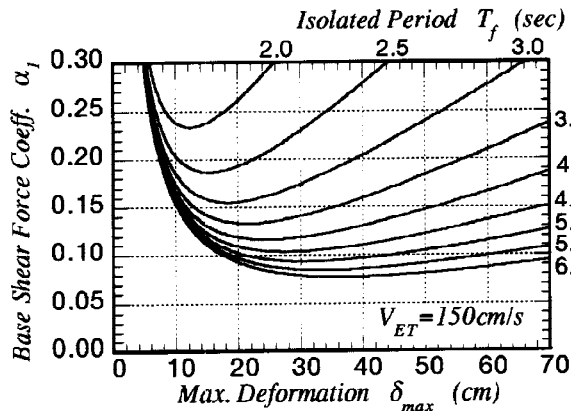


Fig.2 Relationship of $\alpha_1 - \delta_{max}$

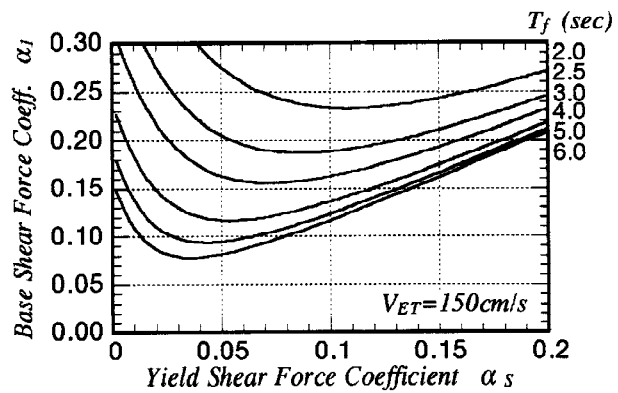
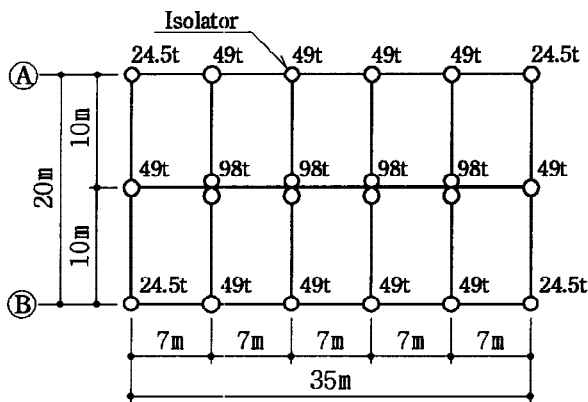
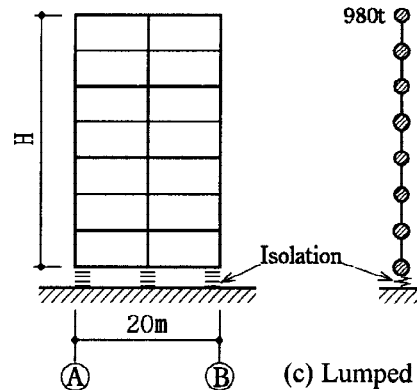


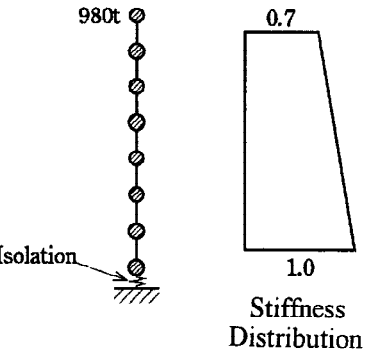
Fig.3 Relationship of $\alpha_1 - \alpha_s$



(a) Plan



(b) Elevation



(c) Lumped Mass Model

Fig.4 Analytical Model

story's weight is the same at 980ton (1.4×700). The target buildings are modeled as the lumped mass model (sway model). The stiffness distribution of the superstructure is trapezoidal as shown in Fig.4(c). Each story's stiffness is established as $T_1 = 0.025H$, when the superstructure's first period (non-isolated) is T_1 and the total height of the building H (unit=m). The height of each story is a uniform 4.0m. For number of stories (N), 5 variations are set: 5, 10, 15, 20, 25 stories. The restoring force characteristics of superstructure set to elastic model. The viscous damping of superstructure is 2% of the critical damping, and the viscous damping of isolating story is 0%. The damping matrix is created as a stiffness proportional matrix.

Rubber Bearings and Dampers

The axial force of rubber bearing is obtained by multiplying the column axial force on one floor as shown in Fig.4(a) by the number of floors. From Fig.4(a), the axial force is classified into three types. A total of 22 rubber bearings are positioned, two below the four columns in the central part and one below the other columns. One type (size) of rubber bearing is used for each building model. The diameter of the rubber bearings are derived in accordance with the aim of achieving an average compressive stress $\bar{\sigma}$ of about 100kg/cm^2 . The restoring force characteristics is modeled based on the experimental results of the compressive shearing tests. Fig.5 shows the relationship between shear strain and shear stress when the compressive stress is 200kg/cm^2 and 300kg/cm^2 . The specimen is 500mm in diameter, 3.75mm in a rubber thickness and 26 rubber layers ($S_1=33.3$, $S_2=5$). S_1 is the first shape factor, defined by the ratio of the cross sectional area to the force-free area of one rubber layer (equal to the conventional shape factors). S_2 is the second shape factor, defined by the ratio of the diameter to the total rubber thickness. It has been found that a certain range of S_2 exists, which may not affect the change of the rubber bearing's horizontal stiffness in relation to fluctuations in the axial load; moreover, will maintain the compressive load support capacity without buckling even at the large deformation. This S_2 range is given by $S_2 \geq 5$. In this analysis, S_2 of the rubber bearing is set as 5. From Fig.5, the restoring force characteristics of rubber bearing is modeled as tri-linear model. The initial shear modulus is 4kg/cm^2 . The linear characteristics is kept until 260% in shear strain, which is equivalent to the half of the diameter of rubber bearing. The breaking shear strain of the specimen lies over 400% regardless of the compressive stress. The shear stiffness K_H of rubber bearing can be calculated by the following equation.

$$K_H = \frac{GA}{h} = \frac{\pi}{4}GS_2 \cdot D \quad (13)$$

where, G : Shear modulus, A : Sectional area ($= \pi D^2/4$), h : Total rubber thickness, $S_2 = D/h$

The rubber bearing diameter D , the stiffness, and the isolated period T_f are shown in Table 1. For dampers, hysteresis dampers are used. The dampers have the perfect elasto-plastic restoring force characteristics. The yield deformation δ_y is 3cm. The yield shear force coefficient α_s is set less than the half of diameter in the maximum

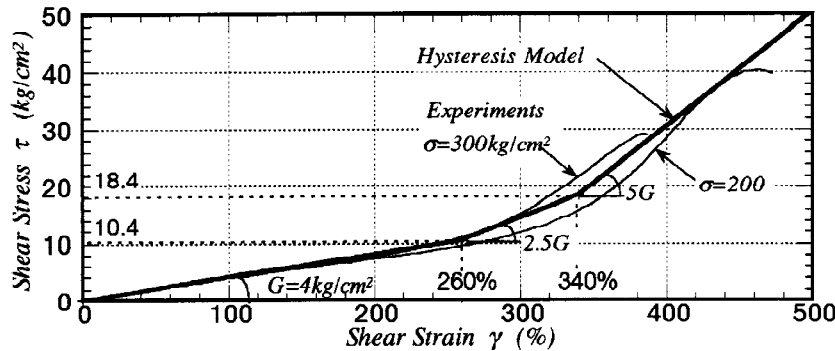


Fig.5 Restoring Force Characteristics of Rubber Bearing

Table 1 Analytical Model

N	W (ton)	H (m)	T_1 (sec)	D (cm)	$\bar{\sigma}$ (kg/cm ²)	K_H (t/cm)	δ_1 (cm)	δ_2 (cm)	δ_{cr} (cm)	T_f (sec)	T_f/T_1
5	5880	20	0.5	60	95	0.94	31.2	40.8	48.0	3.38	6.76
10	10780	40	1.0	80	97	1.26	41.6	54.4	64.0	3.96	3.96
15	15680	60	1.5	100	91	1.57	52.0	68.0	80.0	4.28	2.85
20	20580	80	2.0	110	98	1.73	57.2	74.8	88.0	4.67	2.34
25	25480	100	2.5	125	95	1.96	65.0	85.0	100.0	4.88	1.95

δ_1 is equal to 260%, δ_2 is equal to 340% and δ_{cr} is equal to 400% in shear strain.

deformation ($\delta_{\max} < D/2$). If the δ_{\max}^{opt} in Eq.(11) is below the half of the rubber bearing diameter ($D/2$), α_s^{opt} in Eq.(12) is used. And, except for this condition, α_s is calculated by substituting $\delta_{\max} = D/2$ into Eq.(10).

Input Seismic Wave

For the input seismic waves used in this analysis, artificial seismic waves are created for the design energy spectra shown by Kitamura *et al.* (1992a). The energy input levels (equivalent velocity) V_{EI} of the energy spectra are set to $V_{EI} = 150, 200, 250, 300\text{cm/s}$. For the phase characteristics of the artificial seismic waves, the seismic wave phases recorded during the 1978 earthquake off the coast of Miyagi Prefecture are used. Fig.6 shows the acceleration response spectra, velocity response spectra and energy spectra. Fig. 7 shows the input waveform for $V_{EI} = 200\text{cm/s}$. The maximum acceleration of the input waves is 262.3gal for $V_{EI} = 150\text{cm/s}$; 313.4gal for $V_{EI} = 200\text{cm/s}$; 365.7gal for $V_{EI} = 250\text{cm/s}$; and 403.0gal for $V_{EI} = 300\text{cm/s}$. The input wave duration is 81.92sec.

ANALYSIS RESULTS AND CONSIDERATIONS

Fig. 8 shows the maximum acceleration response for non-isolated (fixed base) structures with 150, 200, 300cm/s in the energy input V_{EI} . Acceleration response become larger as the energy input V_{EI} increased. The amplification of acceleration response is 2 to 3-fold in spite of the natural period of analytical model. For the energy input $V_{EI} = 200\text{-}300\text{cm/s}$, the base shear force coefficient is about 0.4-0.8. It needs the big resistant capacity (force) of structures to maintain the elastic response. Similarly, Fig.9 shows the acceleration response for base-isolated models. The yield shear force coefficient α_s is calculated by substituting $V_{ET} = V_{EI}$ into Eq.(12). In this figure, the factor b_s defined as follows, is shown, which is a important parameter related to the higher mode response.

$$b_s = K_0 / K_s \tag{14}$$

where, K_s : Damper's stiffness, K_0 : Stiffness of the first story of superstructure

The acceleration response with $V_{EI} = 150\text{cm/s}$ shows the uniform response about 150-200gal. In the case of $V_{EI} = 200\text{-}300\text{cm/s}$, the acceleration response at upper stories is much larger than that of $V_{EI} = 150\text{cm/s}$. Especially, for the low height model, the acceleration response at lower and upper stories is bigger than that of middle story. In order to design the maximum deformation less than the allowable deformation against a large earthquake, it need to increase the yield strength of damper. This contribute to increase the damper's stiffness K_s , and the ratio b_s in Eq. (14) become small. Therefore, the contribution of the second mode in the acceleration response is high, and the response at upper and lower story is amplified. But, the maximum acceleration of base-isolated model is much smaller than that of non-isolated model. Table 2 shows the analytical results and the design values of the maximum

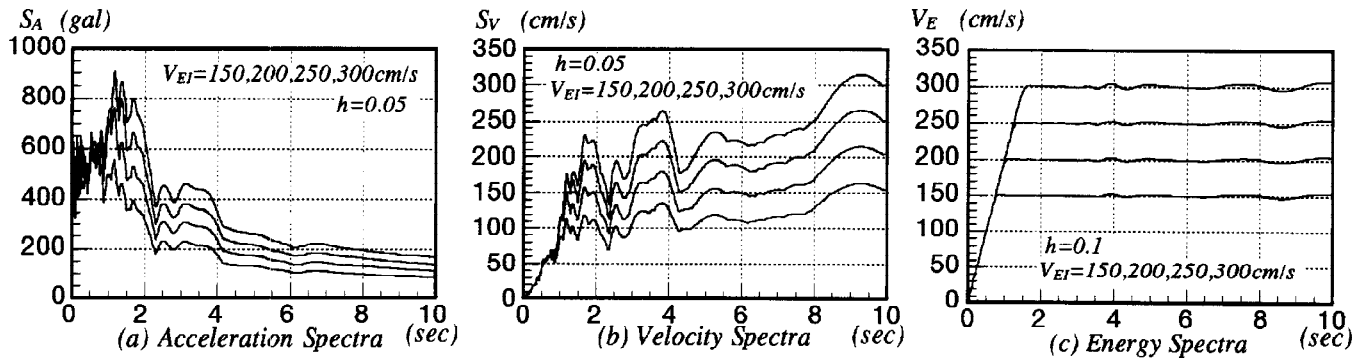


Fig.6 Response Spectra of Input Seismic Waves

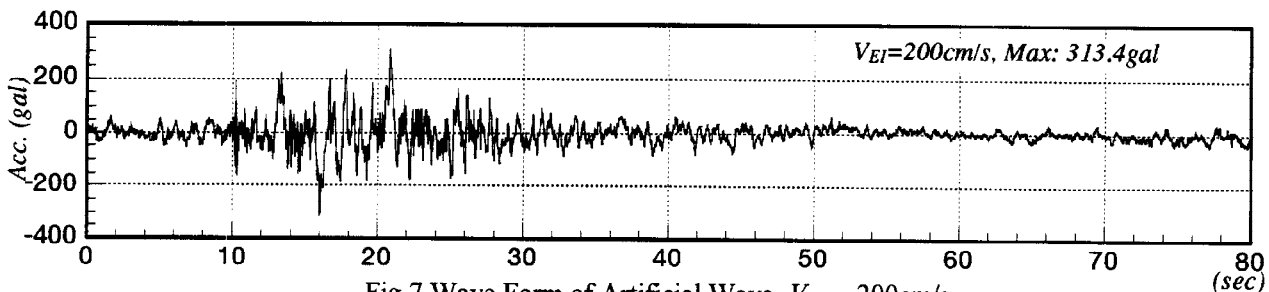


Fig.7 Wave Form of Artificial Wave $V_{EI} = 200\text{cm/s}$

deformation and the base shear force coefficient. The deformation δ_{AVE} is the average deformation of the isolating story, calculated by following equation.

$$\delta_{AVE} = \frac{|\delta_{max}^+| + |\delta_{max}^-|}{2}, \quad \delta_{max} = \max(|\delta_{max}^+|, |\delta_{max}^-|) \quad (15)$$

where, $\delta_{max}^+, \delta_{max}^-$: Maximum deformation in positive and negative directions

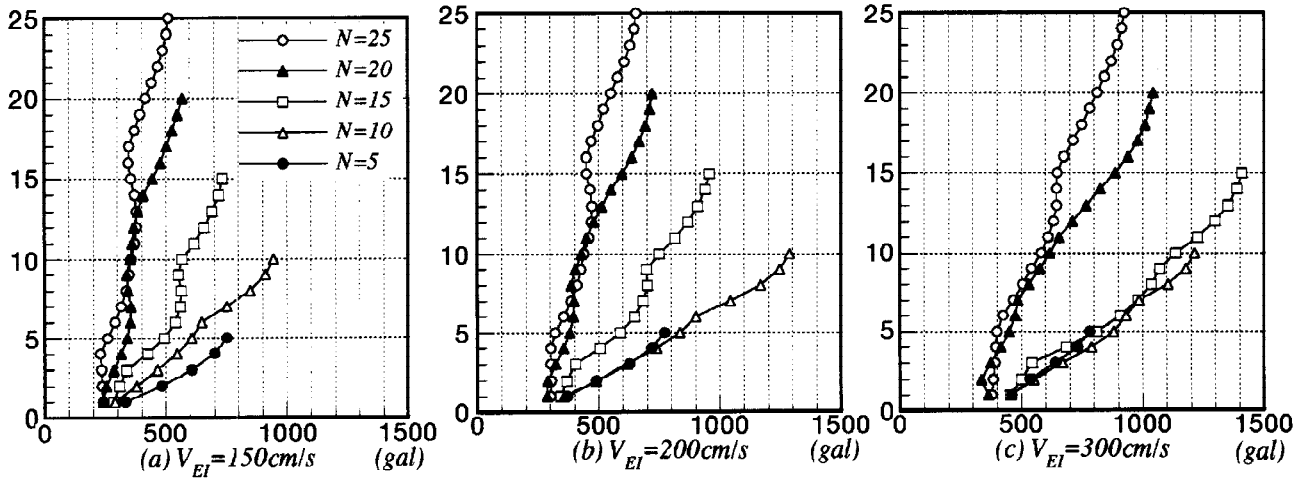


Fig.8 Max. Acceleration Response of Non-Isolated Model

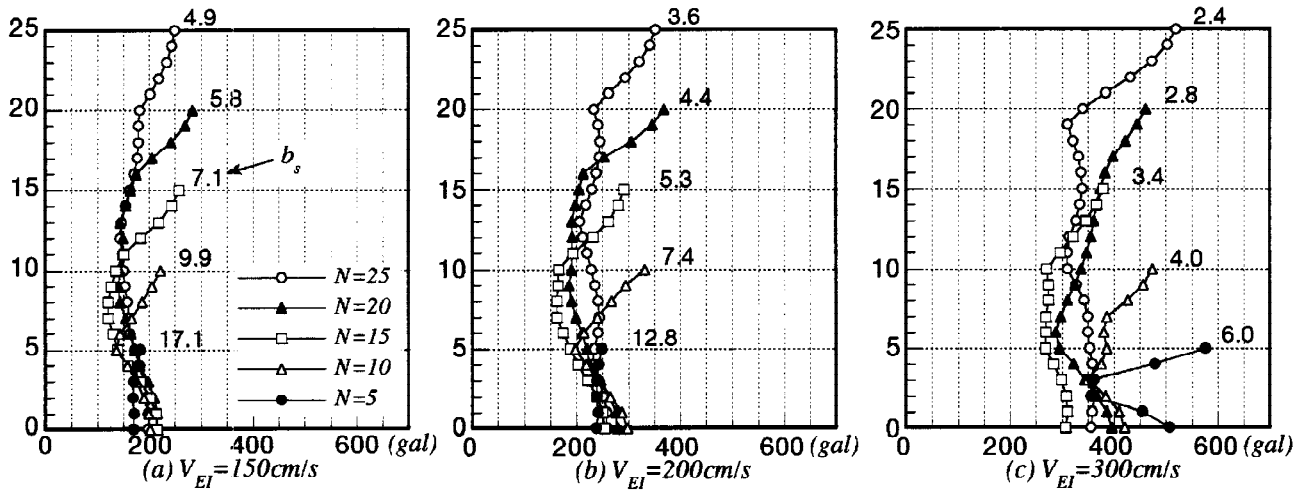


Fig.9 Max. Acceleration Response of Base-Isolated Model

Table 2 Design, Analysis and Prediction Response of the Isolating Story

V_{EI} (cm/s)	N	c_s	Design			Analysis Results				Prediction
			α_1^{opt}	δ_{max}^{opt} (cm)	V_{ET} (cm/s)	κ	α_1	δ_{max} (cm)	δ_{AVE} (cm)	δ_{max} (cm)
150	5	0.0643	0.138	20.8	146	5.46	0.167	29.1	25.7	27.3
	10	0.0549	0.118	24.4	148	6.98	0.116	24.0	22.6	26.8
	15	0.0508	0.109	26.4	143	8.40	0.112	27.7	24.2	23.1
	20	0.0465	0.100	28.8	155	8.68	0.126	42.9	33.7	28.5
	25	0.0445	0.095	30.1	150	8.08	0.125	47.1	34.6	29.8
200	5	0.0857	0.184	27.8	183	5.40	0.240	36.2	33.9	32.8
	10	0.0732	0.157	32.5	183	6.40	0.164	35.6	32.2	33.4
	15	0.0677	0.145	35.2	194	9.56	0.147	36.0	30.0	28.3
	20	0.0620	0.133	38.4	209	9.04	0.161	53.9	43.5	37.5
	25	0.0594	0.127	40.1	201	8.66	0.161	60.0	45.4	37.7
300	5	0.1847	0.290	30.0	244	9.62	0.327	34.9	28.6	16.8
	10	0.1371	0.240	40.0	270	4.56	0.351	56.3	46.6	53.3
	15	0.1079	0.218	50.0	290	8.56	0.217	49.7	49.3	44.1
	20	0.0980	0.200	55.0	316	9.34	0.261	69.7	58.1	52.8
	25	0.0890	0.191	60.2	298	8.90	0.267	81.0	65.6	54.1

In this table, the prediction value of the maximum deformation is also shown, which is calculated by Eq.(6) with the analyzed values of V_{EI} and κ . The analysis value of κ varied from 4.56 to 9.56, but the average of κ is 7.96, which is suited to the proposed value by Akiyama (1989, 1992a). The maximum base shear coefficient is 0.14-0.24 with $V_{EI} = 200\text{cm/s}$ and 0.2-0.36 with $V_{EI} = 300\text{cm/s}$. These values are less than half in the case of non-isolated model. When the number of story N is 15 or less, the analyzed maximum deformation show a good correspondence to the design values, while N is 20 or more, the analyzed deformation is about 1.5 times the design values. This tendency does not depend on the energy input V_{EI} , and is caused by deviating from the assumption in energy based design to increase the flexibility of superstructure. Therefore, if the ratio of the isolated period T_f to the fixed-base period T_1 is 3 or more, the prediction method based on energy balance is very useful. Moreover, it is found that the factor of b_s needs over 10 in order to reduce to effect of the second mode response. The axial force of rubber bearing is fluctuated by over turning moment. Here, the fluctuation of the axial force, which is caused by over turning moment in a longitudinal direction, is considered. If one design condition is that uplift (tension) force should not affect the rubber bearing, the over turning moment's limit M_{cr} is given by $W/4 \times 20$; where W is total weight of superstructure. Fig.10 shows the analytical value and the limit of over turning moment. With the energy input $V_{EI} = 150\text{cm/s}$, the maximum over turning moment does not exceed the limit M_{cr} when the number of story is below 15 (aspect ratio is 3). But, in other case, the maximum over turning moment exceed the limit M_{cr} . If the layout of the rubber bearing would be improved and the axial force would be concentrated (see Fig.11), the limit of over turning moment is $2M_{cr}$. Even with a larger aspect ratio, the over turning moment will not reach the limit of $2M_{cr}$.

Next, the dynamic analysis using the original model designed by the energy input of $V_{EI} = 150\text{cm/s}$ is carried out with input level of $V_{EI} = 200, 250, 300\text{cm/s}$. Fig.12 shows the maximum acceleration response. When the number of story is over 10, the response of $V_{EI} = 250\text{cm/s}$ is slightly bigger than that of $V_{EI} = 150\text{cm/s}$. For $V_{EI} = 300\text{cm/s}$, the acceleration response became larger. Table 3 shows the analytical and predicted values of the maximum deformation and the base shear force coefficient. As the input level V_{EI} is large, the maximum deformation reached the hardening area of rubber bearing. When the input level V_{EI} is 200cm/s , the predicted values in the case of $N \geq 20$ is underestimated like $V_{EI} = 150\text{cm/s}$ shown in Table 2. On the other hand, when V_{EI} is over 250cm/s , the predicted values is overestimated, because the damping capacity of the structure does not correspond to the amount of energy input. The maximum deformation is below 400% in shear strain even in the case of $V_{EI} = 300\text{cm/s}$. Therefore, the rubber bearing don't reach the broken deformation. The base shear force coefficient is 0.2-0.44, which is 2-3 times that in $V_{EI} = 150\text{cm/s}$. If the strength of the superstructure is much enough, the safety of the structure is kept even in the case of input level V_{EI} of 300cm/s . Consequently, the structural safety of base isolated building is kept against the 4 times energy input, if the design is adequate to the large earthquake.

CONCLUSIONS

In this paper, the dynamic analysis of base-isolated structure is carried out and the validity of the prediction method based on the energy balance is discussed. The following conclusions can be drawn from this study:

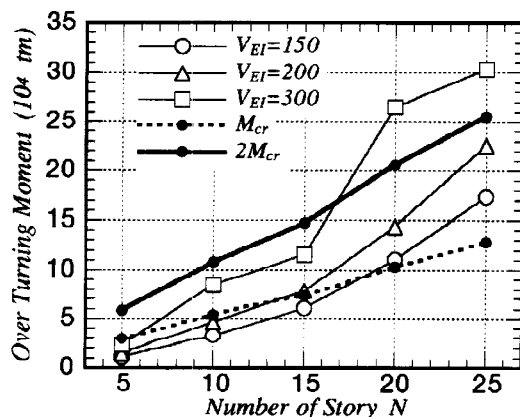


Fig.10 Max. Over Turning Moment of Base-Isolated Model

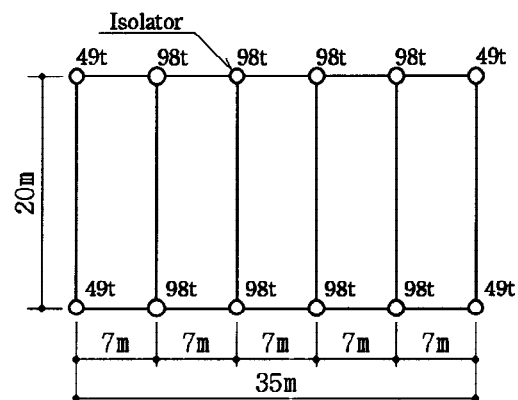


Fig.11 Improved Layout of Rubber Bearing

- 1) The maximum acceleration response of base-isolated building below half that of fixed base structure, even with the high raised buildings.
- 2) The response prediction method based on energy balance is valid in the case of $T_f/T_1 \geq 3$, where, T_f is the isolated period and T_1 is the superstructure's period.
- 3) In order to decrease adequately the effect of second mode response in acceleration response, it is necessary to increase the ratio b_s of the superstructure's stiffness to the damper's stiffness by 10 or more.
- 4) The safety margin of the isolating story's deformation is over 2 times the supposed input energy level V_E until rubber bearings are damaged.

REFERENCES

- Akiyama, H. (1985), Earthquake-Resistant Limit-State Design for Buildings, *Univ. of Tokyo Press*
- Akiyama, H. (1989), Prediction for Seismic Responses of Flexible-Stiff Mixed Structures with Energy Concentration in the First Story, *Trans. of A.I.J. of Constr. Engrg.*, No.400
- Kitamura, H. and Akiyama, H. (1992a), Seismic Response Prediction for Base-Isolated Building by Considering the Energy Balance, *Int. Workshop on Recent Developments in Base-Isolation Techniques for Buildings*, Tokyo
- Akiyama, H. and Kitamura, H. (1992b), Design Energy Spectra for Specific Ground Conditions, *Int. Workshop on Recent Developments in Base-Isolation Techniques for Buildings*, Tokyo

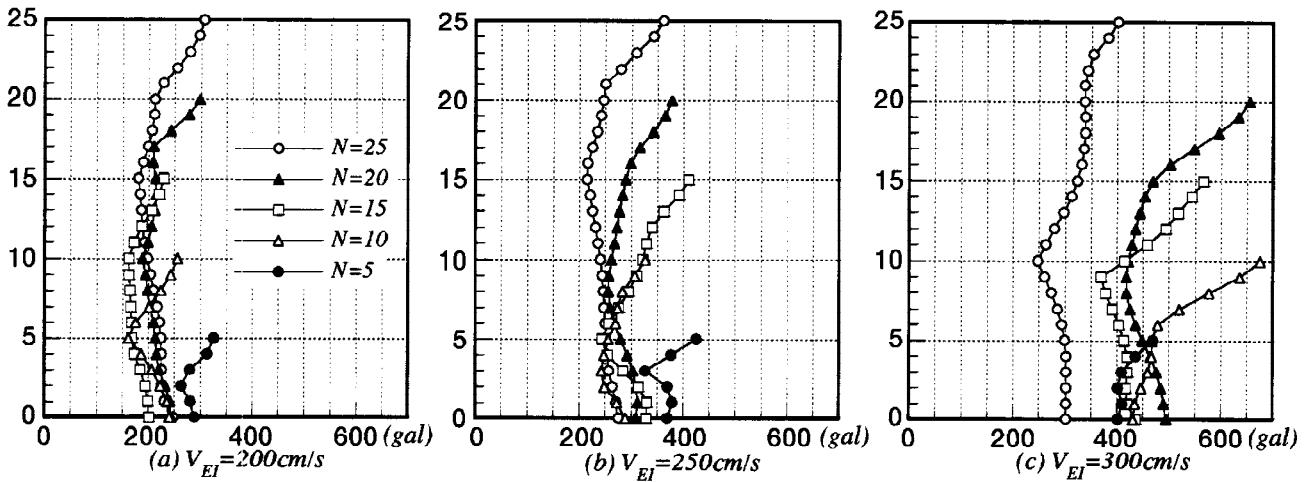


Fig.12 Max. Acceleration Response with Unexpected Seismic Motion

Table 3 Design, Analysis and Prediction Response of the Isolating Story

V_{EI} (cm/s)	N	Design α_s	Analysis Results					Prediction δ_{max} (cm)
			V_{ET} (cm/s)	κ	α_1	δ_{max} (cm)	δ_{AVE} (cm)	
200	5	0.0643	192	6.36	0.252	40.0	35.8	39.0
	10	0.0549	197	11.60	0.146	35.6	34.7	29.4
	15	0.0508	188	8.76	0.157	48.0	39.9	37.1
	20	0.0465	196	9.26	0.148	54.9	50.4	41.8
	25	0.0445	185	9.68	0.132	51.5	46.0	37.7
250	5	0.0643	232	7.76	0.322	44.3	40.9	46.1
	10	0.0549	246	11.50	0.250	55.0	50.4	44.8
	15	0.0508	245	10.26	0.244	66.2	61.1	52.9
	20	0.0465	235	5.28	0.202	68.1	62.9	83.7
	25	0.0445	222	5.10	0.152	63.3	58.6	83.1
300	5	0.0643	291	14.68	0.398	48.7	48.2	42.1
	10	0.0549	303	12.26	0.442	69.8	65.2	61.2
	15	0.0508	298	5.08	0.324	74.4	74.3	102.3
	20	0.0465	283	5.60	0.312	83.3	76.3	102.3
	25	0.0445	259	5.56	0.222	80.8	70.4	98.2